Detection of Hemodynamically Significant Coronary Artery Stenosis: Incremental Diagnostic Value of Dynamic CT-based Myocardial Perfusion Imaging[1]

Fabian Bamberg, MD, MPH
Alexander Becker, MD
Florian Schwarz, MD
Roy P. Marcus, BS
Martin Greif, MD
Franz von Ziegler, MD
Ron Blankstein, MD, MPH
Udo Hoffmann, MD, MPH
Wieland H. Sommer, MD
Verena S. Hoffmann, PhD
Thorsten R. C. Johnson, MD
Hans-Christoph R. Becker, MD
Bernd J. Wintersperger, MD
Maximilian F. Reiser, MD
Konstantin Nikolaou, MD

Purpose: To determine the feasibility of computed tomography (CT)-based dynamic myocardial perfusion imaging for the detection of hemodynamically significant coronary artery stenosis, as defined with fractional flow reserve (FFR).

Materials and Methods: Institutional review board approval and informed patient consent were obtained before patient enrollment in the study. The study was HIPAA compliant. Subjects who were suspected of having or were known to have coronary artery disease underwent electrocardiographically triggered dynamic stress myocardial perfusion imaging. FFR measurement was performed within all main coronary arteries with a luminal narrowing of 50%–85%. Estimated myocardial blood flow (MBF) was derived from CT images by using a model-based parametric deconvolution method for 16 myocardial segments and was related to hemodynamically significant coronary artery stenosis with an FFR of 0.75 or less in a blinded fashion. Conventional measures of diagnostic accuracy were derived, and discriminatory power analysis was performed by using logistic regression analysis.

Results: Of 36 enrolled subjects, 33 (mean age, 68.1 years ± 10 [standard deviation]; 25 [76%] men, eight [24%] women) completed the study protocol. An MBF cut point of 75 mL/100 mL/min provided the highest discriminatory power (*C* statistic, 0.707; $P < .001$). While the diagnostic accuracy of CT for the detection of anatomically significant coronary artery stenosis (>50%) was high, it was low for the detection of hemodynamically significant stenosis (positive predictive value [PPV] per coronary segment, 49%; 95% confidence interval [CI]: 36%, 60%). With use of estimated MBF to reclassify lesions depicted with CT angiography, 30 of 70 (43%) coronary lesions were graded as not hemodynamically significant, which significantly increased PPV to 78% (95% CI: 61%, 89%; $P = .02$). The presence of a coronary artery stenosis with a corresponding MBF less than 75 mL/100 mL/min had a high risk for hemodynamic significance (odds ratio, 86.9; 95% CI:17.6, 430.4).

Conclusion: Dynamic CT-based stress myocardial perfusion imaging may allow detection of hemodynamically significant coronary artery stenosis.

Supplemental material: *http://radiology.rsna.org/lookup/suppl/doi:10.1148/radiol.11110638/-/DC1*

[1] From the Departments of Clinical Radiology (F.B., F.S., R.P.M., W.H.S., T.R.C.J., H.C.R.B., B.J.W., M.F.R., K.N.) and Cardiology (A.B., M.G., F.v.Z.), Ludwig-Maximilians University, Klinikum Grosshadern, Marchioninistrasse 15, 81377 Munich, Germany; Cardiac MR PET CT Program, Department of Radiology, Massachusetts General Hospital, Harvard Medical School, Boston, Mass (F.B., U.H.); Department of Radiology, Brigham and Women's Hospital, Harvard Medical School, Boston, Mass (R.B.); and Institute of Biomedical Epidemiology, Ludwig-Maximilians University, Munich, Germany (V.S.H.). Received March 27, 2011; revision requested May 2; final revision received May 9; accepted May 9; final version accepted May 17. **Address correspondence to** F.B. (e-mail: *fbamberg@post.harvard.edu*).

Despite having an excellent diagnostic accuracy for the detection of obstructive and nonobstructive coronary artery diseases (CADs), cardiac computed tomography (CT) remains a limited test for evaluating the physiologic significance of many anatomic lesions (1). While there is growing evidence that coronary CT angiography may be useful in several clinical scenarios (2), assessment of the hemodynamic significance of coronary stenosis, either noninvasively with the use of myocardial perfusion imaging or invasively with techniques such as fractional flow reserve (FFR), plays a pivotal role in risk stratification and selection of appropriate patients for coronary revascularization (3,4).

Over the past several years, preliminary studies have shown that detection of myocardial perfusion defects under rest (5–7) and stress conditions (8–11) may be feasible by using CT. Despite the promising results of these early studies, they were limited by the absence of quantitative techniques, as well as by the acquisition of images during a predefined single point during early myocardial perfusion. On the other hand, dynamic techniques for evaluating myocardial perfusion imaging—most commonly with magnetic resonance (MR) imaging, positron emission tomography, or, recently, CT (12,13)—may allow for noninvasive quantification of myocardial blood flow (MBF), which may further improve identification of hemodynamic relevance of luminal stenosis (14).

We therefore sought to determine the feasibility of CT-based dynamic myocardial perfusion imaging for the detection of hemodynamically significant coronary artery stenosis as defined by FFR. Our hypothesis was that dynamic assessment of MBF may improve the diagnostic accuracy of cardiac CT for the detection of hemodynamically significant coronary artery stenosis.

Advance in Knowledge

- CT-derived estimates of myocardial blood flow provide incremental diagnostic value for the detection of hemodynamically significant coronary artery stenosis, as defined by invasive fractional flow reserve measurement with a significant increase in discriminatory power (*C* statistic, 0.75–0.90; $P < .001$).

Materials and Methods

Bayer Schering Pharma (Berlin, Germany) contributed partial support for this trial, providing an unrestricted research grant. The authors had full control of the data obtained in this trial.

The study was approved by the institutional review board and the Federal Radiation Safety Council (Bundesamt für Strahlenschutz), and all subjects provided written informed consent. This study was Health Insurance Portability and Accountability Act compliant.

In this prospective feasibility study, patients who were referred for invasive angiography because they were suspected of having or were known to have CAD were enrolled. Inclusion criteria included the following: age 50 to 80 years, symptomatic subjects who were scheduled to undergo diagnostic invasive coronary angiography for assessment of CAD, absence of atrial fibrillation or more than six ectopic beats per minute, and ability to perform a 30-second breath hold. Exclusion criteria were as follows: hemodynamically and clinically unstable (angina at rest, malignant arrhythmias) conditions, history of allergy to iodinated contrast material or history of reactive airway disease, history of active hyperthyroidism among subjects older than 60 years of age, serum creatinine levels greater than 1.5 mg/dL [132.6 μmol/L], atrioventricular block type II and III, and sick sinus syndrome, pregnant or breast-feeding women, and metformin treatment that could not be discontinued after CT. Any treatment with β-adrenergic blocking agents and/or nitrates was discontinued prior to the scanning.

All image acquisitions were performed by using a fast dual-source CT system (Somatom Definition Flash; Siemens Healthcare, Forchheim, Germany) with a collimation of $64 \times 2 \times 0.6$ mm and flying-focal spot, resulting in 2×128 sections. Patient preparation included administration of two antecubital intravenous catheters and placement of electrocardiographic electrodes on the patient's chest, as well as a detailed explanation of the imaging procedure, including practicing of breath holds. No β-adrenergic blocking agent was administered prior to scanning.

The protocol (Fig E1 [online]) included prospective coronary CT angiography in 0.75-mm sections to visualize the coronary arteries under baseline conditions, followed by a dynamic stress acquisition in 3-mm sections over a period of 30 seconds to visualize the myocardium.

Implication for Patient Care

- The use of quantitative dynamic CT-based myocardial perfusion imaging may allow for accurate assessment of the hemodynamic relevance of coronary artery stenosis and therefore may allow a better guide to clinicians in their decision making about the need for invasive angiography and appropriate revascularization strategies.

Published online
10.1148/radiol.11110638 **Content code:** CA

Radiology 2011; 260:689–698

Abbreviations:
CAD = coronary artery disease
CI = confidence interval
FFR = fractional flow reserve
MBF = myocardial blood flow
MBV = myocardial blood volume
NPV = negative predictive value
PPV = positive predictive value
RCA = right coronary artery

Author contributions:
Guarantors of integrity of entire study, F.B., K.N.; study concepts/study design or data acquisition or data analysis/interpretation, all authors; manuscript drafting or manuscript revision for important intellectual content, all authors; approval of final version of submitted manuscript, all authors; literature research, F.B., F.v.Z., R.B., W.H.S., T.R.C.J., H.C.R.B., M.F.R.; clinical studies, F.B., A.B., R.P.M., M.G., T.R.C.J., H.C.R.B., K.N.; experimental studies, F.B., A.B., F.S., R.P.M., M.G., W.H.S., T.R.C.J., B.J.W.; statistical analysis, F.B., R.P.M., U.H., V.S.H.; and manuscript editing, F.B., A.B., F.S., R.P.M., F.v.Z., R.B., U.H., W.H.S., V.S.H., H.C.R.B., B.J.W., M.F.R., K.N.

Potential conflicts of interest are listed at the end of this article.

After obtaining the standard scout image of the entire chest (100 kV), contrast agent timing was determined by administering a test bolus of 15 mL (flow rate, 5 mL/sec) of contrast medium (Ultravist 370; Bayer Schering Pharma) followed by administration of 20 mL of saline, with a power injector (Stellant; Medrad, Indianola, Pa). Subsequently, image acquisition time for coronary CT angiography was determined by adding 4 seconds to the time of peak contrast enhancement in the ascending aorta to allow for adequate contrast enhancement of the coronary arteries. Dynamic myocardial perfusion imaging was started 4 seconds before the arrival of the contrast medium bolus in the ascending aorta.

Standard prospective CT angiography was triggered at 200 msec in the craniocaudal direction by using the following scan parameters: 2 × 100 kVp tube voltage (120 kVp in subjects with a body mass index of ≥30 kg/m^2), 320 mAs per rotation, and 0.28-second gantry rotation time.

Myocardial perfusion imaging was initiated 2 minutes after administration of adenosine (Adrekar; Sanofi, Munich, Germany) at 0.14 mg/kg/min. Data were acquired for 30 seconds with both tubes set at 100 kV, a gantry rotation time of 0.28 second, and a total tube current of 300 mAs per rotation. Two alternating table positions were used in the electrocardiographically triggered mode, with the table moving forward and backward between the two positions (eg, "shuttle mode," with table acceleration of 300 mm/sec^2). Given a detector width of 38 mm, and a 10% overlap between both imaging ranges, the imaging coverage of the acquisition was 73 mm. For a heart rate of 63 beats per minute or less every single heartbeat and for a heart rate of greater than 63 beats per minute every second heartbeat, images were acquired, resulting in a total of 14–15 data sets. A total of 50 mL of iodinated contrast agent (Ultravist 370; Bayer Schering Pharma) was injected at a flow rate of 5 mL/sec, followed by a saline chaser, with the same power injector as mentioned before. On completion of the imaging, adenosine administration was discontinued.

Image analysis was performed on an off-line workstation by using a commercially available dedicated software tool (Leonardo; Siemens Medical Solutions, Erlangen, Germany) by two independent experienced observers. The effective radiation dose was derived by multiplying the dose-length product with the conservative constant k (k = 0.017 mSv/mGy/cm).

Evaluation of the presence of significant coronary artery stenosis was performed on axial source images in a consensus reading by two experienced investigators (F.B. and K.N., with >6 and >8 years of cardiac CT experience, respectively) by using a modified 17-segment model of the coronary artery tree (15). Readers were blinded to the subject's clinical presentation and history. If a consensus could not be reached, a third expert reader determined the final diagnosis (H.C.R.B., with >10 years of cardiac CT experience). The presence of coronary artery stenosis was defined as a luminal obstruction of greater than 50% diameter. If image quality did not permit definite exclusion of a significant stenosis (owing to the presence of motion artifacts, calcification, or low contrast-to-noise ratio), the segment was classified as indeterminate and was counted as positive for the presence of significant coronary artery stenosis.

Perfusion images were reconstructed with a 3-mm section width every 2 mm by using a smooth convolution kernel (B30) and then processed on a standard workstation (Syngo VPN; Siemens Healthcare, Forchheim, Germany). MBF and mean Hounsfield units were determined in each of the 16 myocardial segments, excluding the apical segment (16). A 1-mm subendocardial zone directly adjacent to the contrast material–filled left ventricle and a 1-mm subepicardial zone were excluded from analysis, and a region of interest of 2.5 cm^2 was manually placed in a representative area of each myocardial segment. To estimate MBF, a dedicated parametric deconvolution technique, which was based on a two-compartment model of intra- and extravascular space, was used to fit the time-attenuation curves (17).

To ensure the accurate matching of myocardial segments with the associated vascular territory, blood vessel dominance was used to decide which vessel supplied the inferior and inferoseptal territories.

All patients underwent conventional coronary angiography, using standard equipment (Siemens Medical Solutions, Forchheim, Germany), with a catheter inserted via the femoral artery by using a 6- or 7-F guiding catheter. All angiograms were analyzed by two experienced cardiologists (A.B. and M.G., with >10 and >4 years of experience, respectively); these cardiologists independently analyzed the images for the presence of a significant coronary artery stenosis (≥50% luminal narrowing).

FFR was measured with a sensor-tipped 0.014-inch guidewire (Pressure Wire; Radi Medical Systems, Uppsala, Sweden) in every lesion with a luminal narrowing between 50% and 85% (maximum of two per subject). After positioning the pressure sensor distal of the stenosis, maximal myocardial hyperemia was induced with a continuous intravenous infusion of adenosine in a femoral vein at an infusion rate of 140 μg per kilogram of body weight per minute for a minimum of 2 minutes. During maximum hyperemia, FFR was calculated as the ratio of the mean distal pressure, measured by the pressure wire, divided by the mean proximal pressure measured by the guiding catheter. A coronary artery stenosis of 50% or greater with an FFR value of 0.75 or less or a luminal stenosis of 85% or greater was considered functionally significant (18,19). If more than one coronary artery stenosis was present within the same perfusion territory, the most severe stenosis was considered for analysis.

Demographics, traditional risk factors, and prevalence of coronary artery stenosis depicted with coronary CT angiography are presented as means ± standard deviations and percentages for categorical variables. The intraclass correlation coefficient was used to determine the agreement of measurement of MBF between two observers. A paired t test and repeated-measures analysis of

variance was used to compare MBF and myocardial blood volume (MBV) between coronary arteries, as well as between segments, which were and were not associated with a hemodynamically significant coronary artery stenosis and according to CT stenosis category. To determine whether the observed difference between these territories was independent of heart rate during the scan, age, sex, and body mass index, we fitted linear regression models by using the MBF as the predictor of interest. The MBF cut point was derived by maximization of the *C* statistic by using logistic regression modeling (20). The asymptotic 95% confidence intervals (CIs) for the *C* statistic were estimated by using a nonparametric approach, which is closely related to the jackknife technique proposed by DeLong et al (21).

To determine the accuracy of coronary CT angiography for the detection of hemodynamically significant coronary artery stenosis, we calculated conventional measures of diagnostic accuracy (sensitivity, negative predictive value [NPV], specificity, and positive predictive value [PPV]) by using the previously derived cut point of MBF as a positivity criterion. We accounted for the clustered nature of the myocardial territories per subject by estimating the observed distribution (95% CIs) according to Zhou et al (22). The McNemar test was used to compare measures of diagnostic accuracy between groups. Also, we compared the discriminatory power (*C* statistic as derived with logistic regression analysis) of conventional CT angiography and the CT angiography supplemented by information on myocardial perfusion for the detection of hemodynamically significant coronary artery stenosis similarly by using the standard error of the test statistics as derived from the asymptotic variance covariance (21). Finally, we performed multivariate logistic regression modeling to examine the relative risk associated with the presence of any perfusion deficit (threshold level, 75 mL/100 mL/min) and the presence of hemodynamically significant coronary artery stenosis, defined with FFR. This model was additionally adjusted for age, sex, and history of CAD.

A two-sided *P* value of less than .05 was considered to indicate a significant difference. All analyses were performed by using software (SAS, version 9.1; SAS Institute, Cary, NC).

Figure 1

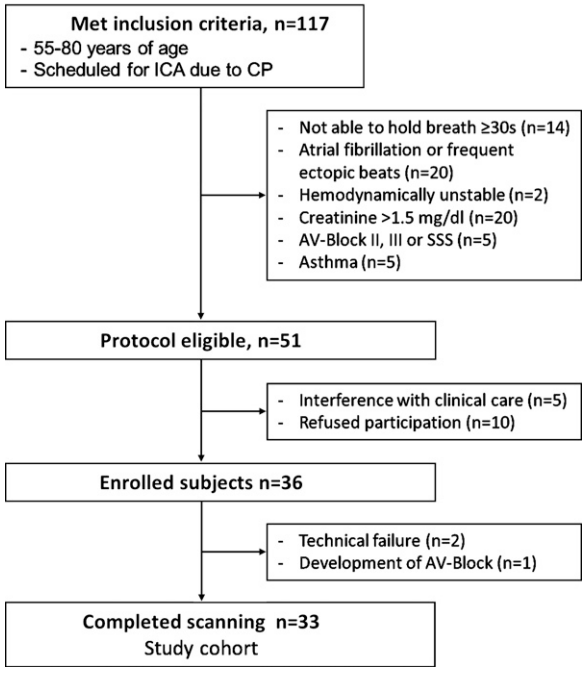

Figure 1: Study flow diagram detailing screening, enrollment, and scanning procedures for the study cohort. Creatinine level in Système International units is >132.6 μmol/L. *AV* = atrioventricular, *CP* = chest pain, *ICA* = invasive coronary angiography, *SSS* = sick sinus syndrome.

Results

Over a study period of 10 months, 117 study participants met the inclusion criteria, and of these, 51 subjects were protocol eligible (Fig 1). Among 36 enrolled subjects, in two, imaging protocols were not completed because of technical failure, and in one, the imaging protocol was interrupted because of developing arrhythmia (atrioventricular block) during adenosine administration; no further adverse event occurred. Thus, 33 subjects formed the study cohort. They were predominantly older men (mean age, 68.1 years ± 10 [standard deviation]; 25 [76%] men and eight [24%] women); patient demographics and risk factors are detailed in Table E1 (online).

On average, the mean duration of the CT protocol was 36 minutes ± 7. The mean effective radiation exposure of CT angiography and myocardial perfusion were 3.1 mSv ± 1 and 10.0 mSv ± 2 (Table E2 [online]), respectively. The mean heart rate significantly increased from 72.2 beats per minute ± 17 at baseline to 83.1 beats per minute ± 16 with adenosine administration ($P < .001$). Among all, 33% (11 of 33) of the perfusion studies provided incomplete coverage of the myocardium, with either partially covered inferior ($n = 10$) or anterior ($n = 1$) wall segments. In addition, five perfusion studies (15%) had impaired image quality because of motion artifacts and required additional postprocessing. These studies were not excluded from the analysis. Intra- and interobserver agreement for MBF and MBV was high, with intraclass correlation coefficients of 0.81 and 0.80, respectively.

At coronary CT angiography during adenosine infusion, of 528 coronary segments, a significant coronary artery stenosis was detected in 46 segments (8.7%). Twenty-one segments (4.0%) were nonevaluable, and they were counted positive for significant coronary artery stenosis, resulting in a total of 67 segments with significant coronary artery stenosis (mean, 12.7%; two stenoses

Measures of Diagnostic Accuracy of Cardiac CT Angiography and MBF for Detection of Anatomically and Hemodynamically Significant Coronary Artery Stenoses

Basis of Measurement	Sensitivity	Specificity	PPV	NPV
	Anatomically Significant Coronary Artery Stenosis (Luminal Narrowing > 50%)			
Per coronary segment	94 (58/62) [84, 98]	97.4 (454/466) [96, 99]	83 (58/70) [72, 91]	99.1 (454/458) [98, 100]
Per coronary vessel	91 (49/54) [80, 96]	69 (29/42) [53, 82]	79 (49/62) [67, 88]	85 (29/34) [69, 95]
	Hemodynamically Significant Coronary Artery Stenosis (FFR ≤ 0.75)			
Per coronary segment	100 (34/34) [89, 100]	92.7 (458/494) [91, 95]	49 (34/70) [36, 60]	100 (458/458) [99, 100]
Per coronary segment plus MBF	91 (31/34) [76, 98]	98.2 (485/494) [97, 99]	78 (31/40) [61, 89]	99.4 (485/488) [98, 100]
Per coronary vessel	100 (29/29) [88, 100]	51 (34/67) [39, 63]	47 (29/62) [36, 57]	100 (34/34) [89, 100]
Per coronary vessel plus MBF	93 (27/29) [77, 99]	87 (58/67 [76, 94]	75 (27/36) [58, 88]	96.7 (58/60) [88, 99]
Per subject	100 (22/22) [85, 100]	18 (2/11) [2, 51]	71 (22/31) [52, 86]	100 (2/2) [15, 100]
Per subject plus MBF	95 (21/22) [77, 100]	64 (7/11) [31, 89]	84 (21/25) [64, 95]	88 (7/8) [47, 99]

Note.—Data are percentages. Numbers in parentheses were used to calculate the percentages. Percentages were rounded. Numbers in square brackets are 95% CIs as percentages. The MBF was CT based.

per subject), predominantly in the right coronary artery (RCA) (n = 22). On a per-patient basis, 31 of 33 (94%) subjects had a significant coronary artery stenosis.

All 33 subjects who completed CT scanning underwent invasive angiography and FFR measurement without an adverse event. The prevalence of morphologically significant coronary artery stenosis was high (63 of 528 segments [11.9%], 54 of 96 vessels [56%], and 31 of 33 subjects [94%] with significant coronary artery stenosis) (Table E1 [online]). In contrast, with FFR, we determined that only a fraction (33 of 63, 52%) of significant coronary artery stenoses were hemodynamically significant (FFR ≤ 0.75).

Overall, myocardial segments pertaining to hemodynamically significant coronary artery stenosis had significantly lower mean MBF and MBV than did segments pertaining to vessels without stenosis (73.2 mL/100 mL/min ± 26 vs 104.8 mL/100 mL/min ± 34 and 16.0 mL/100 mL/min ± 7 vs 19.6 mL/100 mL/min ± 5, for MBF and MBV, respectively) ($P < .001$ for both). Logistic regression analysis revealed a significantly higher discriminatory power for MBF than for MBV (C statistic, 0.78 versus 0.67; $P < .001$). Thus, MBF was selected for analysis of diagnostic relevance. The predicted difference in MBF between ischemic and nonischemic myocardial segments persisted after adjusting for age, sex, body mass index, and difference in heart rate (β, 35.0 mL/100 mL/min; 95% CI: 27.7, 42.2; $P < .001$). The best cutoff of MBF for the differentiation between hemodynamically significant and nonsignificant coronary artery lesions was 75 mL/100 mL/min (C statistic, 0.707; $P < .001$), and it was also confirmed in the subpopulation of subjects with a stenosis. Applying this threshold level resulted in 22.0% (114 of 519) ischemic myocardial segments, 33% (32 of 96) ischemic vessels, and 73% (24 of 33) subjects with hemodynamically significant coronary artery stenosis.

The diagnostic accuracy of CT for the detection of significant coronary artery stenosis (≥50% luminal narrowing as defined with conventional coronary angiography) on a per-segment basis was high (Table 1): sensitivity, 94% (95% CI: 84%, 98%); specificity, 97.4% (95% CI: 96%, 99%); PPV, 83% (95% CI: 72%, 91%); and NPV, 99.1% (95% CI: 98%, 100%). Measurements of diagnostic accuracy on a per-vessel basis are provided in the Table and were similarly high.

Because of the lower prevalence of hemodynamically significant coronary artery stenosis (33 of 528, 6.2%), the PPV for the detection of hemodynamically significant coronary artery stenosis (as defined with FFR ≤ 0.75) on a per-segment basis was moderate (49%; 95% CI: 36%, 60%). When the information on MBF was used to reclassify lesions, 30 of 70 (43%) coronary artery lesions were classified as not hemodynamically significant, resulting in increased PPV (78% [31 of 40]; 95% CI: 61%, 89%; P = .02); three lesions were incorrectly classified as not hemodynamically significant (sensitivity, 91% [31 of 34]; 95% CI: 76%, 98%). These subjects had a lower mean heart rate increase under stress (5.1 beats per minute ± 1 vs 12.4 beats per minute ± 5, P = .06), and 33% (two of three) showed an insufficient coverage of the myocardium. Similar findings were observed on a per-vessel and per-subject basis (Table 1). One subject whose lesion was incorrectly classified as not hemodynamically significant as defined with FFR on a per-patient basis (NPV, 88%) had a higher mean MBF as compared with that of all other subjects (107.3 ± 13 mL/100 mL/min vs 97.9 ± 37 mL/100 mL/min, respectively; P = .03) and thus had a value above the applied threshold level of 75 mL/100 mL/min. Representative cases are shown in Figures 2–8.

By using logistic regression analysis, the discriminatory power of cardiac CT without perfusion information was high (C statistic, 0.753; 95% CI: 0.69, 0.81; $P < .001$). When the information on MBF was used to reclassify lesions, the predictive power was significantly higher

Figure 3

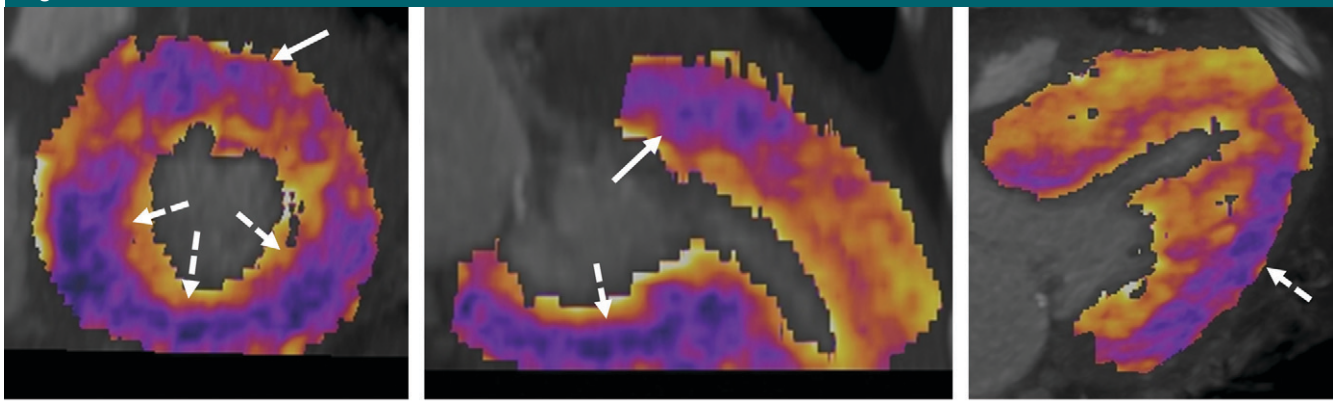

a. b. c.

Figure 3: Color-coded dynamic perfusion CT images **(a)** in short axis, mid ventricle, **(b)** in long axis, and **(c)** in four-chamber views in same patient as in Figure 2 demonstrate significantly reduced myocardial perfusion (42 mL/100 mL/min) in the inferior and inferolateral wall (dashed arrows, darker [more purple] areas) related to the RCA and left circumflex coronary artery, as well as reduced MBF (55 mL/100 mL/min) in the anterior wall related to the left anterior descending coronary artery (solid arrow). Both the left anterior descending and left circumflex coronary artery lesions were determined to be hemodynamically significant at FFR measurement, with FFR of 0.71 and 0.69, respectively.

Figure 2

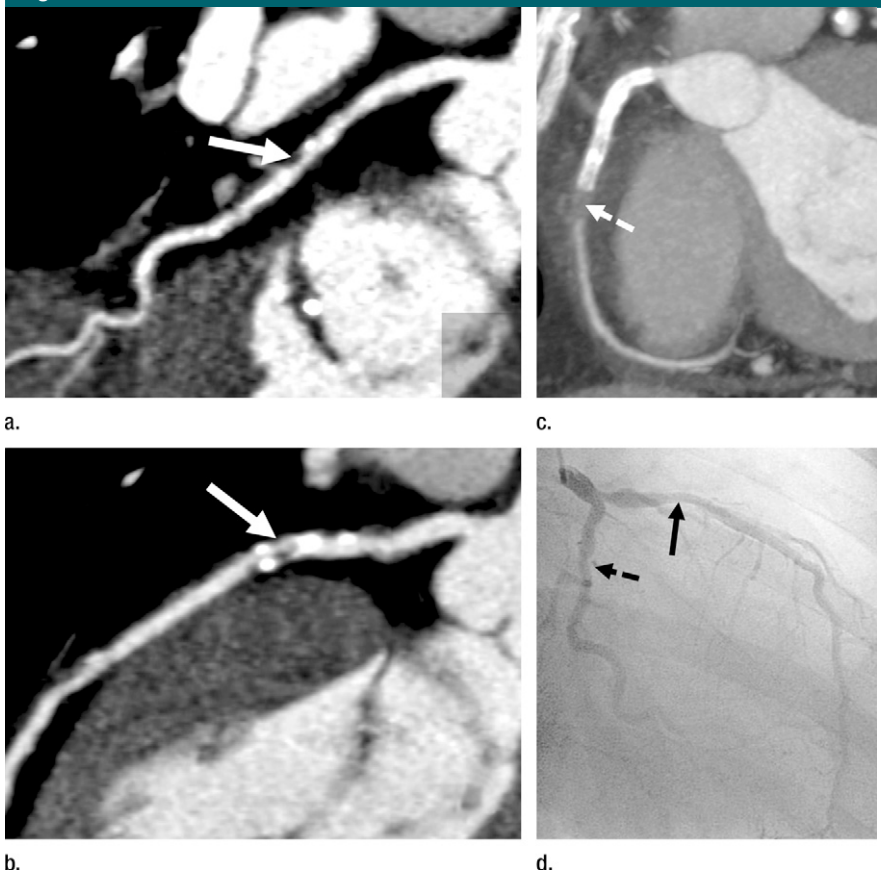

a. c.

b. d.

Figure 2: Coronary CT angiograms demonstrate moderate stenosis (arrow) in **(a)** proximal segment of left circumflex coronary artery, **(b)** calcified and noncalcified plaque (arrow) in the proximal left anterior descending coronary artery, with moderate luminal narrowing, and **(c)** stent in the proximal portion of the RCA and significant high-grade stenosis (arrow) distal to the stent in 67-year-old woman who had chronic chest pain and history of coronary artery stenosis, with subsequent stent placement in the proximal RCA. **(d)** Invasive angiogram in same patient shows moderate stenosis, similarly depicted as on CT angiograms, in the left circumflex coronary artery (dashed arrow) and left anterior descending coronary artery (solid arrow).

(*C* statistic, 0.898; 95% CI: 0.83, 0.96; $P < .001$; predicted difference, 0.15; 95% CI: 0.07, 0.22). The presence of a coronary artery stenosis with a corresponding MBF of less than 75 mL/100 mL/min was associated with an approximately 90-fold higher risk for a hemodynamically significant coronary artery stenosis (odds ratio, 86.9; 95% CI: 17.6, 430.4).

Discussion

In the present feasibility study, we showed that dynamic adenosine-stress myocardial perfusion CT can help quantify MBF in addition to providing an anatomic

Figure 5

a. b. c.

Figure 5: Color-coded dynamic perfusion CT **(a)** short-axis, **(b)** long-axis, and **(c)** four-chamber views in same patient as in Figure 4 reveal homogeneous MBF in the left anterior descending coronary artery, left circumflex coronary artery, and RCA territories (107 vs 98 vs 102 mL/100 mL/min, respectively).

Figure 4

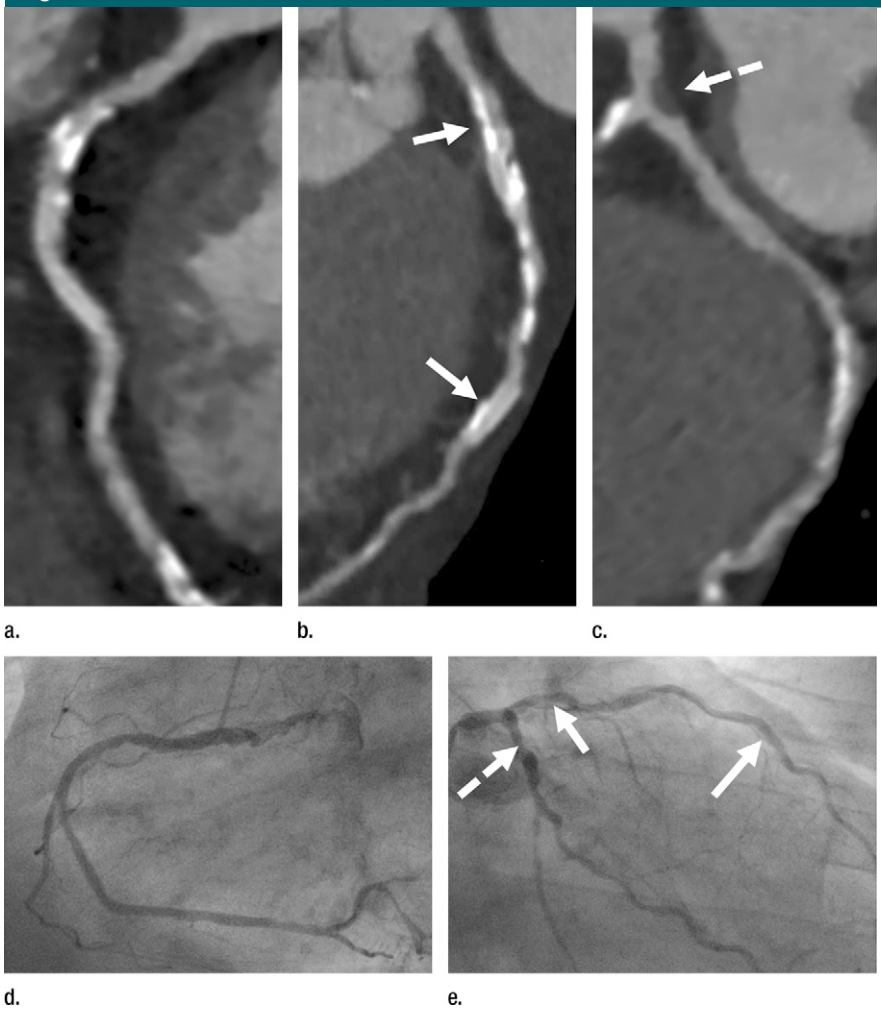

a. b. c. d. e.

Figure 4: **(a–c)** Curved multiplanar reconstructions in 71-year-old man show extensive atherosclerotic plaque in **(a)** left anterior descending coronary artery, **(b)** RCA, and **(c)** left circumflex coronary artery. In the proximal segment of the RCA, a significant coronary artery stenosis (solid arrows, **b**) could not be excluded because of substantial calcification, and in the left circumflex coronary artery, there is a noncalcified plaque in the proximal segment, causing moderate luminal stenosis (dashed arrow, **c**). **(d, e)** Invasive angiography shows no coronary artery stenosis in **(d)** RCA and confirms **(e)** presence of moderate stenosis in the proximal left circumflex coronary artery (dashed arrow) and mild to moderate stenosis in the proximal and distal segment of the left anterior descending coronary artery (solid arrows).

assessment of coronary artery stenosis. Our data suggest that CT-derived estimates of MBF provide incremental diagnostic value for the detection of hemodynamically significant coronary artery stenosis, as defined with invasive FFR measurement, the currently accepted standard for assessing the hemodynamic significance of coronary artery stenotic lesions (23).

While CT provides a useful noninvasive technique to evaluate coronary artery anatomy, the functional significance of many coronary artery findings is often unclear and may lead to increased downstream test utilization (eg, radionuclide

perfusion imaging, stress MR imaging, or FFR) to help guide treatment decisions (3,24,25). Specifically, Meijboom et al (26) showed that the diagnostic accuracy of a quantitative assessment of coronary artery stenosis with CT was highly correlated with angiographic findings. However, for the detection of hemodynamically significant coronary artery stenosis, as assessed with FFR (26), CT angiography only had a sensitivity of approximately 50%, a finding that is consistent with our observation and with findings in other studies (3,25). In our study, only approximately 50% of significant lesions were hemodynamically significant, thus resulting in a substantial decrease in the PPV.

Our work also extends the prior work by Blankstein et al (8) and Rocha-Filho et al (11) who demonstrated that adenosine-mediated stress can help assess reversible ischemia, with diagnostic accuracy (and radiation exposure) comparable to that with single photon emission computed tomography (SPECT) and provides incremental diagnostic value at CT angiography (8,11). In their analysis, they found a sensitivity of 93% for the detection of significant coronary artery stenosis and a corresponding perfusion defect at SPECT, which is similar to the observed diagnostic accuracy in our cohort (sensitivity, 91% [31 of 34]; PPV, 78% [31 of 40]). However, in contrast to Blankstein et al (8) and Rocha-Filho et al (11), we used a dynamic protocol that permits derivation of a quantitative measure of myocardial perfusion similar to the established CT-based perfusion in brain imaging (27). Investigators who perform further research will need to determine the added value of "dynamic" imaging with MBF quantification to "static" imaging (ie, a single set of images obtained during early myocardial perfusion) and to determine whether the added radiation exposure associated with dynamic imaging can be offset by improved detection of ischemia.

Similar to prior animal studies, we measured the tissue-attenuation curves over time, which were used to calculate MBF, and MBF highly correlated with the established standard of microsphere-derived MBF (r^2 = 0.92) (28). While we selected a region of interest of 2.5 cm^2 to measure MBF in a representative region of the segment, further research will be necessary to determine the optimal method to quantitatively or semiquantitatively assess MBF, also potentially the transmural extent of the perfusion defect (9).

It is important to note that, in our analysis, we determined an MBF of 75 mL/100 mL/min as an ideal cut point, on the basis of maximization of the area under the curve as a criterion. However, this factor may need further validation across different patient populations. For instance, in our study, one subject had an average MBF that was higher than this threshold level and was thus incorrectly categorized as having a nonhemodynamically significant stenosis, which may partly explain the observed tendency of a decreased NPV.

Our results need to be evaluated in the context of a number of study limitations and considerations. Selection bias may be present in our design because recruited subjects generally had a high probability of coronary artery stenosis (ie, history of CAD was present in 85% of subjects), as indicated in Table E1 (online). More important, the PPV and NPV are dependent on the prevalence of disease. Thus, these estimates are valid only for a population with the same prevalence as in this study. Also, our results are based on 33 subjects, and further research will be necessary to confirm these initial observations. Another important limitation of our study is that, in most of the patients with false-negative results, we achieved suboptimal vasodilatory stress and breathing artifacts. Clearly, these observations emphasize the need for adequate preparation, instruction, and dedicated acquisition. Further aspects that will need more attention are as follows: *(a)* The radiation exposure of approximately 12–13 mSv associated with our protocol was higher than the dose associated with contemporary CT angiographic techniques. While this dose, which is equivalent to nuclear techniques with the use of SPECT, is relatively high, it is similar to the dose observed during prior CT perfusion investigations in which dynamic images were not used. *(b)* We found that approximately one-third of scans

Figure 6

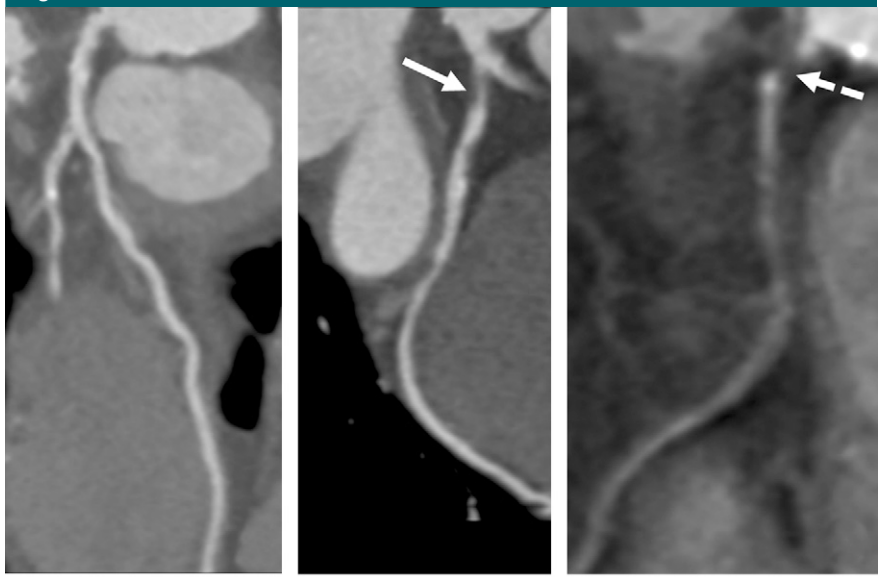

Figure 6: **(a–c)** Curved multiplanar reformats in 65 year-old man with stable angina who had **(c)** significant ostial lesion (arrow) in the RCA (dashed arrow), moderate luminal narrowing in **(a)** middle segment of the left anterior descending coronary artery, and **(b)** moderate stenosis (arrow) in the proximal left circumflex coronary artery.

Figure 7

a. b.

Figure 7: Invasive coronary angiogram in same patient as in Figure 6 demonstrates **(a)** moderate lesion in the proximal left circumflex coronary artery (arrow), which was hemodynamically significant (FFR, 0.67), and **(b)** borderline hemodynamically relevant middle left anterior descending coronary artery lesion (arrow), with an FFR of 0.76.

Figure 8

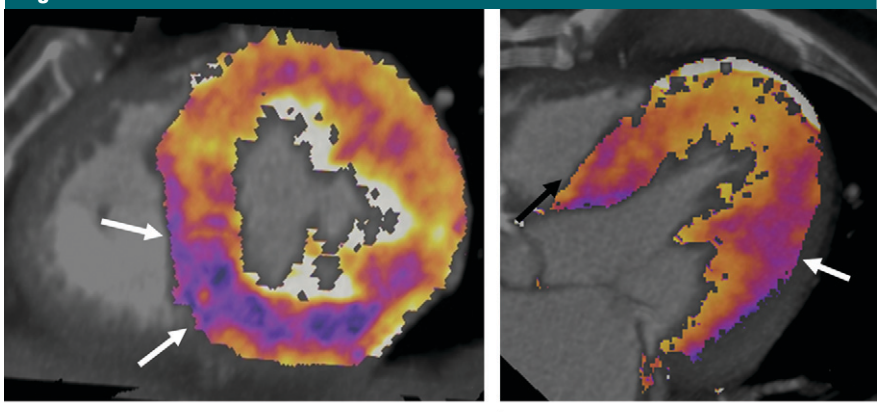

a. b.

Figure 8: Color-coded dynamic myocardial perfusion CT images in same patient as in Figure 6 show **(a)** reduced MBF in the inferior wall (arrow), with a value of 56 mL/100 mL/min, on the short-axis view, **(b)** moderately reduced MBF in the anterior myocardial segment (72 mL/100 mL/min), and reduced MBF in the lateral wall (arrow) corresponding to the hemodynamically significant lesion of the proximal left circumflex coronary artery.

were incompletely covered by the available scan volume of 73 mm. While this coverage may be sufficient to cover the main proximal territories, clearly further technological advances are warranted. *(c)* More important, our study did not include dynamic rest perfusion imaging, as our protocol was designed to minimize the added radiation exposure associated with two dynamic acquisitions. While the dedicated coronary CT angiographic acquisition can potentially be used to assess first-pass myocardial perfusion, the current analysis was designed as an initial step to determine whether information on MBF can help identify hemodynamically significant coronary artery stenosis. Further focused research will be necessary to determine whether CT will allow for differentiation between infarcted and ischemic myocardium by using either first-pass "static," dynamic rest perfusion imaging, or delayed enhancement acquisitions.

In conclusion, our data suggest that a combined assessment of coronary artery anatomy with CT angiography and a dedicated dynamic CT-based stress perfusion imaging to estimate MBF permits accurate identification of hemodynamically significant coronary artery stenosis. Further research will be necessary to confirm the efficacy in large-scale trials for myocardial tissue characterization and clinical effectiveness of the technique.

Disclosures of Potential Conflicts of Interest: **F.B.** Financial activities related to the present article: institution received unrestricted grant from Bayer Schering Pharma. Financial activities not related to the present article: received payment for lectures including service on speakers bureaus from Siemens Medical Solutions. Other relationships: none to disclose. **A.B.** No potential conflicts of interest to disclose. **F.S.** Financial activities related to the present article: none to disclose. Financial activities not related to the present article: received payment for speakers fee from Siemens Healthcare. Other relationships: none to disclose. **R.P.M.** No potential conflicts of interest to disclose. **M.G.** No potential conflicts of interest to disclose. **F.v.Z.** No potential conflicts of interest to disclose. **R.B.** No potential conflicts of interest to disclose. **U.H.** No potential conflicts of interest to disclose. **W.H.S.** No potential conflicts of interest to disclose. **V.S.H.** No potential conflicts of interest to disclose. **T.R.C.J.** Financial activities related to the present article: none to disclose. Financial activities not related to the present article: received honoraria for workshops and lectures from Siemens. Other relationships: none to disclose. **H.C.R.B.** No potential conflicts of interest to disclose. **B.J.W.** Financial activities related to the present article: none to disclose. Financial activities not related to the present article: received payment for lectures including service on speakers bureaus from Siemens Healthcare and Bayer. Other relationships: none to disclose. **M.F.R.** No potential conflicts of interest to disclose. **K.N.** Financial activities related to the present article: institution received unrestricted grant from Bayer Schering Pharma. Financial activities not related to the present article: received payment for lectures including service on speakers bureaus from Bayer Schering Pharma and Siemens Healthcare. Other relationships: none to disclose.

References

1. Budoff MJ, Achenbach S, Blumenthal RS, et al. Assessment of coronary artery disease by cardiac computed tomography: a scientific statement from the American Heart Association Committee on Cardiovascular Imaging

and Intervention, Council on Cardiovascular Radiology and Intervention, and Committee on Cardiac Imaging, Council on Clinical Cardiology. Circulation 2006;114(16):1761–1791.

2. Taylor AJ, Cerqueira M, Hodgson JM, et al. ACCF/SCCT/ACR/AHA/ASE/ASNC/NASCI/SCAI/SCMR 2010 Appropriate use criteria for cardiac computed tomography: a report of the American College of Cardiology Foundation Appropriate Use Criteria Task Force, the Society of Cardiovascular Computed Tomography, the American College of Radiology, the American Heart Association, the American Society of Echocardiography, the American Society of Nuclear Cardiology, the North American Society for Cardiovascular Imaging, the Society for Cardiovascular Angiography and Interventions, and the Society for Cardiovascular Magnetic Resonance. Circulation 2010;122(21):e525–e555. Published October 25, 2010. Accessed November 2010.

3. Tonino PA, De Bruyne B, Pijls NH, et al. Fractional flow reserve versus angiography for guiding percutaneous coronary intervention. N Engl J Med 2009;360(3):213–224.

4. Hachamovitch R, Hayes SW, Friedman JD, Cohen I, Berman DS. Comparison of the short-term survival benefit associated with revascularization compared with medical therapy in patients with no prior coronary artery disease undergoing stress myocardial perfusion single photon emission computed tomography. Circulation 2003;107(23):2900–2907.

5. Nieman K, Shapiro MD, Ferencik M, et al. Reperfused myocardial infarction: contrast-enhanced 64-section CT in comparison to MR imaging. Radiology 2008;247(1):49–56.

6. George RT, Silva C, Cordeiro MA, et al. Multidetector computed tomography myocardial perfusion imaging during adenosine stress. J Am Coll Cardiol 2006;48(1):153–160.

7. Schuleri KH, Centola M, George RT, et al. Characterization of peri-infarct zone heterogeneity by contrast-enhanced multidetector computed tomography: a comparison with magnetic resonance imaging. J Am Coll Cardiol 2009;53(18):1699–1707.

8. Blankstein R, Shturman LD, Rogers IS, et al. Adenosine-induced stress myocardial perfusion imaging using dual-source cardiac computed tomography. J Am Coll Cardiol 2009;54(12):1072–1084.

9. George RT, Arbab-Zadeh A, Miller JM, et al. Adenosine stress 64- and 256-row detector computed tomography angiography and perfusion imaging: a pilot study evaluating the transmural extent of perfusion abnormalities to predict atherosclerosis causing myocardial ischemia. Circ Cardiovasc Imaging 2009;2(3):174–182.

10. Tamarappoo BK, Dey D, Nakazato R, et al. Comparison of the extent and severity of myocardial perfusion defects measured by CT coronary angiography and SPECT myocardial perfusion imaging. JACC Cardiovasc Imaging 2010;3(10):1010–1019.

11. Rocha-Filho JA, Blankstein R, Shturman LD, et al. Incremental value of adenosine-induced stress myocardial perfusion imaging with dual-source CT at cardiac CT angiography. Radiology 2010;254(2):410–419.

12. Bastarrika G, Ramos-Duran L, Rosenblum MA, Kang DK, Rowe GW, Schoepf UJ. Adenosine-stress dynamic myocardial CT perfusion imaging: initial clinical experience. Invest Radiol 2010;45(6):306–313.

13. Bamberg F, Klotz E, Flohr T, et al. Dynamic myocardial stress perfusion imaging using fast dual-source CT with alternating table positions: initial experience. Eur Radiol 2010;20(5):1168–1173.

14. Kajander S, Joutsiniemi E, Saraste M, et al. Cardiac positron emission tomography/computed tomography imaging accurately detects anatomically and functionally significant coronary artery disease. Circulation 2010;122(6):603–613.

15. Austen WG, Edwards JE, Frye RL, et al. A reporting system on patients evaluated for coronary artery disease: report of the Ad Hoc Committee for Grading of Coronary Artery Disease, Council on Cardiovascular Surgery, American Heart Association. Circulation 1975;51(suppl 4):5–40.

16. Cerqueira MD, Weissman NJ, Dilsizian V, et al. Standardized myocardial segmentation and nomenclature for tomographic imaging of the heart: a statement for healthcare professionals from the Cardiac Imaging Committee of the Council on Clinical Cardiology of the American Heart Association. Circulation 2002;105(4):539–542.

17. Bruder H, Raupach R, Klotz E, Stierstorfer K, Flohr T. Spatio-temporal filtration of dynamic CT data using diffusion filters. In: Samei E, Hsieh J, eds. Proceedings of SPIE: medical imaging 2009—physics of medical imaging. Vol 7258. Bellingham, Wash: SPIE–the International Society for Optical Engineering, 2009; 725857.

18. Kern MJ. Coronary physiology revisited: practical insights from the cardiac catheterization laboratory. Circulation 2000;101(11):1344–1351.

19. Pijls NH, De Bruyne B, Peels K, et al. Measurement of fractional flow reserve to assess the functional severity of coronary-artery stenoses. N Engl J Med 1996;334(26):1703–1708.

20. Hanley JA, McNeil BJ. The meaning and use of the area under a receiver operating characteristic (ROC) curve. Radiology 1982;143(1):29–36.

21. DeLong ER, DeLong DM, Clarke-Pearson DL. Comparing the areas under two or more correlated receiver operating characteristic curves: a nonparametric approach. Biometrics 1988;44(3):837–845.

22. Zhou XH, Obuchowski NA, McClish DA. Statistical methods in diagnostic medicine. New York, NY: Wiley-Interscience, 2002.

23. Serruys PW, di Mario C, Piek J, et al. Prognostic value of intracoronary flow velocity and diameter stenosis in assessing the short- and long-term outcomes of coronary balloon angioplasty: the DEBATE Study (Doppler Endpoints Balloon Angioplasty Trial Europe). Circulation 1997;96(10):3369–3377.

24. Shaw LJ, Heller GV, Travin MI, et al. Cost analysis of diagnostic testing for coronary artery disease in women with stable chest pain: Economics of Noninvasive Diagnosis (END) Study Group. J Nucl Cardiol 1999;6(6):559–569.

25. Blankstein R, Di Carli MF. Integration of coronary anatomy and myocardial perfusion imaging. Nat Rev Cardiol 2010;7(4):226–236.

26. Meijboom WB, Van Mieghem CA, van Pelt N, et al. Comprehensive assessment of coronary artery stenoses: computed tomography coronary angiography versus conventional coronary angiography and correlation with fractional flow reserve in patients with stable angina. J Am Coll Cardiol 2008;52(8):636–643.

27. Muizelaar JP, Fatouros PP, Schröder ML. A new method for quantitative regional cerebral blood volume measurements using computed tomography. Stroke 1997;28(10):1998–2005.

28. George RT, Jerosch-Herold M, Silva C, et al. Quantification of myocardial perfusion using dynamic 64-detector computed tomography. Invest Radiol 2007;42(12):815–822.